ISSN 0031-918X, The Physics of Metals and Metallography, 2012, Vol. 113, No. 9, pp. 823–830. © Pleiades Publishing, Ltd., 2012.
Original Russian Text © A.S. Shirinyan, Yu.S. Bilogorodskyy, 2012, published in Fizika Metallov i Metallovedenie, 2012, Vol. 113, No. 9, pp. 867–875.

THEORY OF METALS

Atom–Atom Interactions in Continuous Metallic Nanofilms

A. S. Shirinyan[a] **and Yu. S. Bilogorodskyy**[b]

[a] *Taras Shevchenko National University of Kyiv, pr. Akademika Glushkova 2, Building 1, 03690 Kyiv, Ukraine*
[b] *Bogdan Khmelnitskyy Cherkasy National University, Taras Shevchenko blvd. 81, 18031 Cherkasy, Ukraine*

Received February 2, 2011;
in final form, January 30, 2012

Abstract—Physical reasons of the existence of the nanosystem-size dependence of the potential energy of the neighboring atoms are considered, and a thermodynamic validation of this dependence is given. Solid nanofilms of monoatomic metallic systems having an fcc structure are simulated by the molecular-statics method with the Morse and Sutton–Chen potentials.

Keywords: size effect, interaction potential, molecular statics, continuous film, lattice parameter, atom energy

DOI: 10.1134/S0031918X12090116

1. INTRODUCTION

The problem of describing the effect of dimensions on the properties and stability of nanostructured materials is one of the key problems in modern materials science [1, 2]. In order to solve this problem, it is necessary to understand the behavior and properties of materials at an atomic level. In many cases, the respective solution is constructed on the basis of knowledge of atom–atom interactions, which determine physicochemical properties of systems [3, 4].

It is well known that properties of materials change with size of the system being considered as this size tends to a nanometric scale and as the percentage of surface atoms of nanodispersed systems grows [5]. Multilayer solid metal films obtained by various methods of sputtering atoms onto inert substrates in vacuum facilities [6] form an important class of nanostructured systems. For such systems, the size of objects becomes commensurate with the range of intermolecular-interaction forces; therefore, the energy of atom–atom interaction may also become size-dependent.

This size dependence can readily be understood upon considering that the matter density in a nanodimensional material may differ from its counterpart in massive samples. For spherically symmetric bodies, this may be due, for example, to the change in the Laplace pressure with size and, accordingly, to the change in the average distance between neighboring atoms. This may in turn lead to a change in the surface-energy density [7, 8] and to a decrease or an increase in the potential energy of atom–atom interaction within a nanomaterial. An enhanced concentration of defects in nanomaterials may be yet another factor leading to the size dependence of the potential energy of interaction between neighboring atoms. For example, the presence of vacancies and a change in their concentration may lead to a change in the coordination number of atoms [6]. It follows that, if one applies a thermodynamic description, for example, to a binary nanosystem on the basis of a local-configuration-interaction model [9] belonging to the type of the regular-solution model (where one usually employs the energy of atom–atom interaction), then the need for taking into account the size dependence in question becomes obvious.

At the same time, it is impossible to explain experimentally observed size dependences of, for example, the surface energy via taking into account the curvature of the surface for thin continuous films. This means that the size dependence in question stems from the size-dependent change in the effective pair energy of atom–atom interaction in a nanomaterial both at the surface and in the bulk of the material [10] rather from the effect of the surface curvature. In view of this, it becomes necessary to study the energy dependences of physical quantities in thin films and small systems, and one can do this on the basis of computer models for systems containing about 10^3 to 10^7 atoms.

Various nanocrystal models that purport to explain size effects in nanomaterials have been proposed in recent years. Basically, the proposed explanation relies on taking into account the quantization of the phonon energy, the anharmonicity of lattice vibrations, and the interaction of an atom in the vicinity of a site of the nanomaterial crystal lattice [11]. This approach reveals that size effects manifest themselves within 0.1% for interatomic distances in intervals from about 1 to 10 nm at high temperatures (above the Debye temperature) and disappear as the temperature becomes lower. Without rejecting this possibility, we propose an alternative explanation on the basis of considering optimum energy states of the crystal and a collective effect of the self-organization of nanocrystal atoms. This effect manifests itself in a lattice deformation and in a change in spatial positions of atoms even at zero temperature, in which case there are no atom vibrations.

The basic hypothesis of the present study relies on the idea that there exists a correlation between the size of a metallic nanosystem, the lattice parameter, interatomic distances, and the energies of the interaction of atoms in the bulk of the metal with its crystal lattice. Present-day quantum-mechanical ab initio methods are yet hardly appropriate for studying such systems over long time scales, so that, in testing our hypothesis on the size dependence of physical quantities in nanodimensional systems, it would be reasonable to employ methods of molecular dynamics (MD) and molecular statics (MS) with known interaction potentials for metals [12–15].

The ensuing exposition is organized as follows. First, we discuss available experimental results (Section 2) and frequently used potentials of atom–atom interaction (Section 3). After that, we perform a simple theoretical estimation for the example of an fcc metal (Section 4). An MS model of a solid nanodimensional film for monoatomic systems of fcc metals is formulated in Section 5. The respective results of MS calculations are presented in Section 6. In the last section of this article, we make concluding comments that outline the possibilities for employing the results that we obtained.

2. EXPERIMENTAL DATA

Experimental information about films is quite contradictory, whereas quantitative data for nanoparticles and discontinuous condensates predominantly show a growing decrease in the lattice period as the crystallite size becomes smaller. Such data were obtained for particles of many metals, such as for example, Ag, Au, Bi, and Pt, and for binary crystallites, such as KCl, NaCl, CsI, and NaBr. On the other hand, the lattice parameter for continuous films of Fe, Cu, Ag, Au, γ-Cr, and Pt proved to be increased by 1 to 2%, while the lattice for Al films is normal. The lattice parameter for LiF crystallites 50 to 120 Å in size turned out to be slightly greater than a normal one. A decrease in the lattice constant was obtained for Ag discontinuous films, but no change in the lattice constant was revealed electronographically upon the beginning of continuous-layer formation. Experiments with fine-dispersed globular films of V and Cr showed a substantial dependence of their behavior on the surrounding-medium pressure. It was found that, at a pressure of 10^{-8} mm, the lattice parameter for discontinuous films from touching particles decreased in relation to that in massive samples, but the growth of the lattice parameter with decreasing thickness was recorded at a pressure of 10^{-5} mm Hg. Monte Carlo calculations for fcc structures of argon clusters at 0 K on the basis of data on the radial distribution function showed the growth of the distance between the nearest neighbors in response to a decrease in size [16, 17].

All of the experimental results quoted above show that competing reasons for the change in lattice constants in nanomaterials exist. Moreover, the experimental errors of the instruments used and the uncertainties in the applied procedures are superimposed on special features in the behavior of nanomaterials.

In the majority of the experiment, the nanodimensional metallic films and particles are found to have an fcc structure. For example, electronographic investigations of Ta, Nb, W, and Mo films reveal an fcc structure of average size 5 to 10 nm instead of a conventional bcc structure [16, 17]. For Y, Gd, Tb, Ho, and Tm rare-earth metals, fcc structures were obtained experimentally instead of hcp (as in the case of massive crystals) [18].

In the majority of cases, the values obtained for the lattice parameters in metals can be quite accurately described by a hyperbola-type approximation; that is,

$$a(L) = a_\infty \left(1 + b/L\right), \tag{1}$$

where L is the characteristic size of the nanodimensional system being considered (film thickness h or nanoparticle radius R), a_∞ is the asymptotic value of the lattice parameter for large dimensions, and b is an approximation parameter. In other words, the average density of metals becomes size-dependent.

For nanodimensional materials, experimental results frequently yield a value within 1 to 2% for the relative change in the lattice parameter $\Delta a/a_\infty$ [16–21]. We will now use these results to perform a simple theoretical estimation on the basis of a microscopic model of atom–atom interaction.

3. POTENTIALS OF ATOM–ATOM INTERACTION

An adequate description of the potential of atom–atom interaction is a fundamental problem in simulating strongly interacting nanodimensional systems. The present-day classification of molecular interactions distinguishes three regions of distances. These are (i) short distances, where repulsion dominated by Coulomb and exchange interactions manifest itself; (ii) intermediate distances in the vicinity of the potential minimum, where electrostatic, exchange, and exchange-polarization interactions and charge transfer manifest themselves; and (iii) long distances at the potential tail, where attraction involving electrostatic multipole–multipole, polarization, relativistic magnetic, and retarded electromagnetic interactions manifests itself [22]. A function appropriate for representing atom–atom interaction should meet the following criteria: (a) it should tend asymptotically to a finite value for $r \to \infty$; (b) it should have a minimum at a point $r = r_0$; (c) as the distance tends to $r = 0$, the function in question should increase or tend to infinity; and (d) the allowed eigenvalues of energy in the solution of the Schrödinger equation for the chosen potential should agree with spectroscopic data on the molecules being studied.

Such potentials include the exponential Morse potential, which was proposed in the 1920s. By using spectroscopic data, Morse was able to select potential parameters for a large class of molecules and inert gases in metals [12]. In describing states of solids and properties of cubic crystals, the Morse potential was successfully applied in the studies of Slater, Torrens, and Girifalco and Weizer [23–25], who used experimental values of the latent energy of evaporation, lattice parameter, and compressibility factor.

The Morse potential can be represented in the form [22–28]

$$U_M(r) = U_0\left(\exp\{-2\alpha(r - r_0)\} - 2\exp\{-\alpha(r - r_0)\}\right), \quad (2)$$

where $U_0 = |U_M(r_0)|$ and α are the parameters of, respectively, the dissociation energy for a pair of atoms and the degree of anharmonicity of the potential energy; r_0 is the equilibrium distance between two atoms; $\Delta r = r - r_0$ is the displacement of an atom from the equilibrium position; and r is the distance between the atoms.

The Morse potential function is frequently used to simulate covalent molecules; defects in cubic crystals; and bcc, bcc, and hcp metals and was adequately studied [29–31]. At the same time, it is noteworthy that the redistribution of charges at metal surfaces requires taking into account, in the atom–atom interaction, the Coulomb (ion–electron–ion) component, which is disregarded in many pair potentials, including the Morse potential [32]. Detailed investigations of various authors show that the long-range part of the Morse potential is in poorer agreement with experimental data, since, in this region of distances, an inverse power-law dependence works better than the exponential dependence—moreover, there can even exist oscillation tails in the potential profile [21, 32]. At $r = 0$, the Morse potential is finite, which also constrains the region of its applicability. Nevertheless, it describes satisfactorily vibrational levels of crystals, since the region of distances around the minimum r_0 is of importance for these levels.

Not only is the development of potentials of atom–atom interaction incomplete, but it rather gains momentum in view of the appearance of new computer facilities. According to the opinion of many authors, the Schommers potential based on pseudopotential theory supplemented with a phenomenological description and an effective two-body treatment [33–36] is one of the most promising pair potentials of this kind. The addition of an interaction of the van der Waals type to the Coulomb component makes it possible to describe dipole–dipole and dipole–monopole interactions in some metals. For example, the Schommers potential describes quite correctly the majority of properties of aluminum over a broad temperature range—namely, the melting temperature, diffusion constants in the liquid phase, the structure of bulk solid and liquid phases, and the density of phonon states. This is precisely the reason why this potential has frequently been used in recent years to simulate nanostructures [37].

In the past years, the use of multiparticle potentials—in particular, the Sutton–Chen potential—in which an atom is affected by the "jelly" of close- and far-lying ions and an electron cloud, has become quite efficient [38, 39]. The Sutton–Chen potential has the form

$$U_{SC}(r) = \varepsilon\left(\frac{1}{2}V(r) - c\sqrt{\rho}\right), \quad (3)$$

where $V(r) = \sum_{j=1}^{N}\left(\frac{a}{r_j}\right)^{m_1}$ is a potential that simulates atom interaction with the lattice and which takes into account repulsion induced by the Pauli exclusion principle; $\rho = \sum_{j=1}^{N}\left(\frac{a}{r_j}\right)^{m_2}$ takes into account the local density of atoms in the interaction; c is a dimensionless parameter; ε is a parameter that has dimensions of energy; a is the lattice constant; and m_1 and m_2 are positive integers, $m_1 > m_2$ (usually $m_1 = 9$, $m_2 = 6$).

We will perform the respective analysis both for the case of the Morse potential (2) and for the case of the Sutton–Chen potential (3). A comparison of the results obtained in this way with their counterparts corresponding to different model potentials reveals that, despite quantitative distinctions, the basic result that the properties of nanodimensional materials are size-dependent remains in force. A detailed comparative analysis is beyond the scope of the present article. We will give it in subsequent publications.

4. THEORETICAL ESTIMATION

We will perform theoretical estimations for the example of the Morse pair potential. For the case of a continuous film whose thickness is h, expression (1) makes it possible to estimate readily the spacing between the closest atoms in an fcc metal as $r_{\text{opt}} = a(h)/\sqrt{2}$. Upon substituting the last expression into formula (2) for the potential energy and taking into account the experimental result in (1), we obtain the dependence of the energy of atom–atom interaction

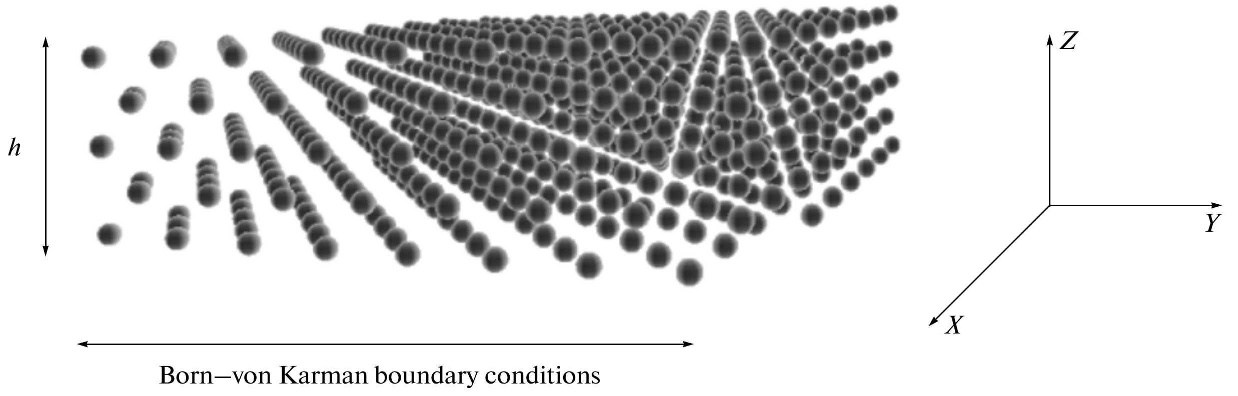

Fig. 1. Multilayer solid metal film with an fcc structure and coordinate frame.

in the first coordination sphere, $\Phi(h) = U_M(r_{\text{opt}})$, as a function of the film thickness; that is,

$$\Phi(h) = U_0\left(\exp\left\{-\frac{2\alpha a_\infty}{\sqrt{2}}\left(1-\frac{r_0\sqrt{2}}{a_\infty}+\frac{b}{h}\right)\right\} - 2\exp\left\{-\frac{2\alpha a_\infty}{\sqrt{2}}\left(1-\frac{r_0\sqrt{2}}{a_\infty}+\frac{b}{h}\right)\right\}\right). \quad (4)$$

Thus, we have obtained the first—and, simultaneously, the main—result of our study: the presence of a size dependence of the energy of atom–atom interaction. A similar consideration can be applied to nanoparticles as well.

It should be noted that the estimate in (4) was obtained in the approximation specified by Eq. (1). Therefore, this estimate is not a perfect validation of the above hypothesis that the energies within the film are size-dependent. The point is that expression (1) can also be considered as the result of an increase in the fraction of surface atoms in nanodimensional materials; allowance for this circumstance by means of averaging may lead to a dependence of the type in (1). In order to prove that the proposed hypothesis of atom–atom interaction is applicable not only to surface atoms but also to atoms in the interior of the film, we perform a MS calculation and separate the effect for surface layers from the effect for internal layers of the nanofilm being considered.

With the aim of analyzing in greater detail thickness-dependent physical properties, we now proceed to perform an MS investigation of nanofilms formed by chosen fcc metals.

5. MS MODEL OF A SOLID NANOFILM

We have constructed a three-dimensional molecular-statics model of a nanofilm from an fcc metal in a vacuum (see Fig. 1).

In order to determine the potential energy of the whole metal-film crystal in which atoms occupy fixed positions, it is necessary to sum the expression for the potential of atom–atom interaction over the material volume. The simplest way to do this consists in choosing one crystal atom for the origin of coordinates [40]. For the case of the Morse potential (2), the total potential energy of a nanodimensional system can be written in the form

$$E_M = \frac{1}{2}U_0\sum_{i=1}^{N}\sum_{j=1}^{N}\left(\exp\{-2\alpha(r_{ij}-r_0)\} - 2\exp\{-\alpha(r_{ij}-r_0)\}\right), \quad (5)$$

where r_{ij} is the distance from the jth atom to the chosen ith atom and j is the number of an atom in the set of neighbors of the ith atom [summation in expression (5) is performed for $i \neq j$].

For the case of the Sutton–Chen potential (3), we accordingly obtain

$$E_{SC} = \varepsilon\sum_{i=1}^{N}\left(\frac{1}{2}\sum_{j=1}^{N}\left(\frac{a}{r_{ij}}\right)^{m_1} - c\sqrt{\sum_{j=1}^{N}\left(\frac{a}{r_{ij}}\right)^{m_2}}\right), \quad (6)$$

where summation is performed for $i \neq j$.

In order to trace the effect of coordination spheres of atom interactions, we will calculate the average potential energy W_n of atom interaction with the whole lattice in the chosen nth layer of the lattice along the Z axis (along the thickness). Within the Morse model, we arrive at the expression

$$W_n = \sum_{j=1}^{r_j<r_{\text{cut}}} U_M(r_j). \quad (7)$$

For the case of the Sutton–Chen potential, we accordingly have

$$W_n = \varepsilon\left[\frac{1}{2}\sum_{j=1}^{r_j<r_{\text{cut}}}\left(\frac{a}{r_j}\right)^{m_1} - c\sqrt{\sum_{j=1}^{r_j<r_{\text{cut}}}\left(\frac{a}{r_j}\right)^{m_2}}\right]. \quad (8)$$

In expressions (7) and (8), summation is performed over all distances r_j smaller than the chosen cutoff radius r_{cut}, which was compared with the equilibrium radius $r_e = a_\infty/\sqrt{2}$ corresponding to the first coordination sphere of atom–atom interaction for a massive fcc sample.

We will use expressions (2), (3), (5)–(8) to test in detail the hypothesis that there exists a correlation between the nanofilm thickness and the energy of atom interaction with the lattice. For this, the procedure of MS minimization of the nanosystem potential energy as given by Eqs. (5) and (6) is used to determine the optimum density and special features of atom–atom interaction in a film that contains N_{lay} layers. In our MS calculations, we changed, in general, the thickness from an eight-atom layer to a 140-atom layer, this corresponding to the thickness range from 1 to 30 nm.

It is noteworthy that a direction that stands out exists in a film—along its thickness (see Fig. 1). Therefore, it was necessary to implement the algorithm of MS optimization of the energy of our system in such a way as to find optimum interatomic distances (lattice periods) along the width, a_Z (in our case, this is the direction of the [100] vector— Z axis) and along the film, a_{XY} (along the [010] or [001] vector— X and Y axes). The interaction of atoms along the (100) plane was specified in the code used with allowance for the Born–von Karman periodic boundary conditions.

6. RESULTS OF MS CALCULATIONS

By and large, the size effect can manifest itself differently for the lattice parameter and for the energy of atom interaction with the lattice. We will show this for films from two fcc metals: Cu and Pb.

Interatomic distances. The results for the distribution of distances between atoms over the film thickness show the presence of internal regions (see Fig. 2) and surface regions, where the crystal lattice undergoes a nonuniform expansion or compression. One can also see that the potentials that we chose lead to different results. While the behavior of internal lattice atoms proves to be of the same type in the two models that we chose (plateau in Fig. 2), the behavior of surface atoms shows opposite trends. According to our calculation on the basis of the Morse model for films containing N_{lay} = 16 layers, for example, the internal regions of the crystal lattice along Z prove to be more compressed in the central region and expanded as one approaches the film surface (Fig. 2). At the same time, the MS calculation with the Sutton–Chen potential shows the compression of the surface layer a_Z.

Most frequently, experimental results may yield only averaged values of the lattice parameter or interplane distances; therefore, it would be reasonable to consider the possibility of determining averaged values of interatomic distances for chosen metals[12, 23–27, 41–46]. Averaging over the entire film makes it possible to find the lattice parameter $\langle a\rangle$ for various thicknesses, as well as a_Z within the film and at the surface (see Fig. 3).

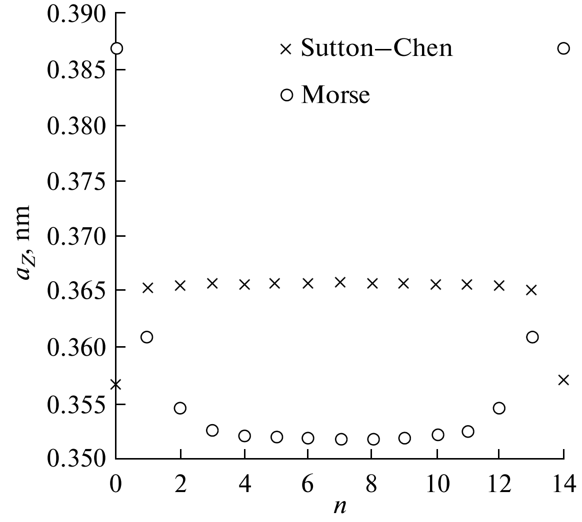

Fig. 2. Results of our molecular-statics calculations within two models for the thickness distribution of a_Z for each layer n (from one surface to the other) in a copper film from N_{lay} = 14 layers. The Morse potential [22] leads to the expansion of surface layers, while the Sutton–Chen potential [38] leads to the compression of the external layer.

One can see that our MS simulation shows the presence of a size effect both in the bulk of the film and in its surface layer (Fig. 3), the effect being different for different directions—that is, the size effect is anisotropic, which manifests itself in the lattice deformation. The Sutton–Chen potential leads to a more pronounced size effect in the surface layer (see Fig. 3b). Moreover, size-dependent changes may be substantially different in internal and surface layers. The averaged pattern of the size dependence of the lattice parameter $\langle a\rangle$ is determined by the dominance of the surface effect.

At the same time, it is of interest not only to consider surface layers but also to trace interatomic distances within the film and to study the energy state of atoms within internal (bulk) layers of the film, since we formulated the basic hypothesis of our study precisely for the bulk layers.

Energy of atom–atom interaction. We will now calculate the energy of atom interaction with the lattice, focusing on internal atoms. For this, we take a copper film by way of example and perform an MS analysis, minimizing the energy (6) of this film. Figure 4a shows the results obtained by calculating the energy W_n on the basis of the Morse potential for a film of $N_{\text{lay}} = 16$ layers with allowance for different numbers of coordination spheres of atom interaction (cutoff radius r_{cut}). The difference in the energy levels W_n at different values of the cutoff radius is due to an increase in the number of atoms contained in the respective coordination sphere

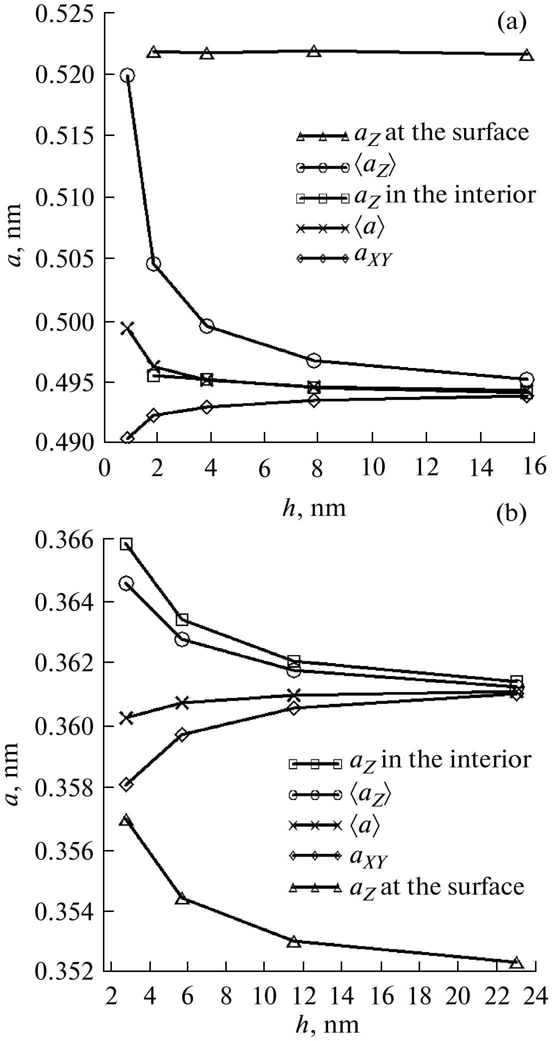

Fig. 3. Comparison of lattice parameters versus the film thickness that were calculated for internal and surface layers by using the chosen potentials at the cutoff radius of $r_{\rm cut} = 4r_{\rm e}$ for (a) lead films treated according to the Morse model [22] and (b) copper films treated according to the Sutton–Chen model [38].

of interaction. It is well known that, in fcc metals, the first, second, and third coordination spheres contain, respectively, 12, 42, and 92 atoms; the total number of neighbors in the *k*th sphere is $10k^2 + 2$ [47].

Let us now calculate the effective potential of interaction between neighboring atoms that are internal with respect to the film, $\Phi(h)$. For this, we determine the average energy of interaction of an internal atom in the middle of the film thickness (Fig. 4b) in the first coordination sphere. As a result, we find that the size effect manifests itself quite well for internal atoms up to film thicknesses of about 30 nm, and this confirms our hypothesis. The respective analysis for spherical metallic particles reveals the presence of the effect up to sizes of about 50 nm.

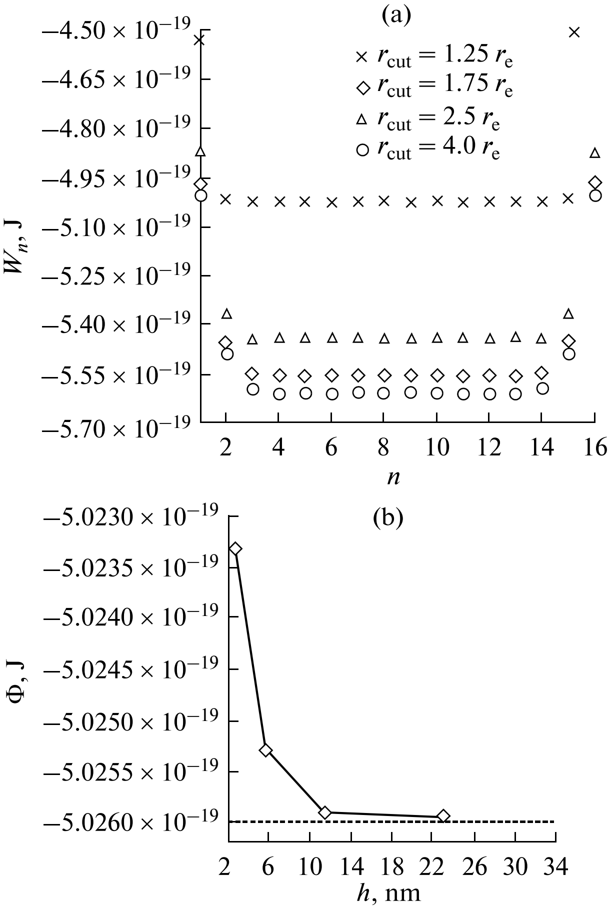

Fig. 4. (a) Energy of atom–lattice interaction in the *n*th layer of a 16-layer copper film for various numbers of coordination spheres taken into account in the calculation based on the Sutton–Chen model [38]; (b) potential energy of the interaction of an internal atom of a copper film with neighboring atoms (in the first interaction sphere) as a function of the nanofilm thickness *h* according to calculations based on the Sutton–Chen model [38].

7. CONCLUDING COMMENTS

Our investigation of the equilibrium state of nanofilms by the method of molecular statics with the Morse and Sutton–Chen potentials has revealed the presence of a size dependence of the lattice parameter, interatomic distances, and the energy of atom–atom interaction both in the interior of a nanodimensional material and at its surface. The effect in question is collective and is due to the fact that, in a thin film, part of the long-range tail of the potential is cut off, which changes the number of atoms in interaction spheres. This result shows that, in order to construct a thermodynamic description of nanodimensional systems, it is necessary to refine energy dependences not only for surface layers but also for volume components of the energy. In particular, it can be assumed that, for a first approximation, effective potentials of the pair interaction of atoms in the interior of continuous nanofilms can be written as an expansion in a Taylor series (see Fig. 4b); that is,

$$\Phi(h) = \Phi_\infty\{1 - \eta/h\}. \tag{9}$$

where Φ_∞ is the potential of atom–atom interaction in the bulk phase (it corresponds to the diagram of state for the respective massive material) and h is the nanofilm thickness. From the above consideration, it is obvious that η depends on the structure type and the sort of atoms and may also depend on the film thickness. According to (9), the properties of the nanomaterial of a continuous film for large thicknesses approach asymptotically their counterparts for massive samples.

Our result makes it possible to refine methods for constructing nanophase diagrams [48]. In particular, we believe that, in employing models of (ideal, regular, or subregular) solutions in the thermodynamics of thin films and condensed nanodimensional systems, the effective potentials of pair atom–atom interaction, $\Phi(h)$, should be modified with allowance for the aforesaid and be taken to be dependent on the size of the system being considered. In our opinion, the respective dependences and potentials can be found from experimental diagrams of state for nanodimensional systems. At the same time, it should be borne in mind that the pair-interaction energies $\Phi(h, x)$ depend on coordinates (see Fig. 4a), so that averaged values of the energies of atoms in the bulk and at the surface of nanodimensional systems will be extracted from phase diagrams.

The results that we obtained for fcc nanofilms show the following: first, the size effect in the energy dependences in question is present for films and particles of small thickness, up to several tens of nanometers; second, the amplitude of such a size effect in the energies for the metals chosen here is modest, amounting to about 1%; and, third, a description of nonuniform systems in terms of energies averaged over the whole sample has limitations associated with surface segregations caused by gradients of energies.

At the same time, the size dependence of energies of atom–atom interaction can make it possible to obtain deeper insight not only into the thermodynamics of nanodimensional systems (change in the conditions of phase equilibrium in nanodimensional materials and shift of curves on phase diagrams) but also into the kinetics of processes proceeding in them (change in the mobility of atoms because of the size dependence of the activation energy for the diffusion of atoms) [49, 50].

ACKNOWLEDGMENTS

The work was performed under the agreement on scientific cooperation between Institute of Electrophysics of Ural Division of RAS and Educational-Scientific Centre "Physicochemical Material Science" of Taras Shevchenko Kiev National University and Ukrainian NAS (agreement from 01.07.2011) and Project of the Centre "Physicochemical Material Science" (agreement K-4-65 from 01.07.2011, PK 0110U008212, OK 0211U005630, IK 0711U010360).

REFERENCES

1. R. A. Andrievskii and A. M. Glezer, "Size Effects in Nanocrystalline Materials: II. Mechanical and Physical Properties," Phys. Met. Metallogr. **89**, 83–104 (2000).
2. H. Gleiter, "Nanostructured Materials: State of the Art and Perspectives," Nanostruct. Mater. **6**, 3–14 (1995).
3. K. Binder, P. Nielaba, and V. Pereyra, "Phase Coexistence in Binary Mixtures in Thin Films with Symmetric Walls: Model Calculations for Two- and Three-Dimensional Ising Lattices," Z. Phys. B **104**, 81–98 (1997).
4. E. A. Shunikov, Yu. P. Khukhryanskii, and I. N. Arsent'ev, "Using Axisymmetric Potential in Modeling Crystal Growth from Melt," Tech. Phys. Lett. **31**, 173–175 (2005).
5. A. S. Shirinyan and V. A. Makara, "Topical Problems of Nanomaterials and Nanotechnologies," Nanosist. Nanotekhnol. Nanomater. **8**, 223–269 (2010).
6. N. T. Gladkikh, S. V. Dukarov, A. P. Krishtal', V. N. Larin, V. N. Sukhov, and S. I. Bogatyrenko, *Surface Phenomena and Phase Transformations in Condensed Films* (Kharkov. Nat. Univ., Kharkov, 2004) [in Russian].
7. Q. Jiang, H. M. Lu, and M. Zhao, "Modeling of Surface Energy of Elemental Crystals," J. Phys.: Condens. Matter **16**, 521–530 (2004).
8. M. N. Magomedov, "Dependence of the Surface Energy on the Size and Shape of a Nanocrystal," Phys. Solid State **46**, 954–968 (2004).
9. B. Ya. Pines, *Essays on Metal Physics* (Kharkov. Gos. Univ., Kharkov, 1961) [in Russian].
10. A. S. Shirinyan and Yu. S. Bilogorodskyy, "Influence of the Size Dependence of the Atomic Interaction Energy in Nanosystems on the Shift of Equilibrium Boundaries on Phase Diagrams of Continuous Binary Bi–Sn Nanofilms," Vestnik Cherkassk. Nat. Univ., Ser. Fiz.–Mat., No. 171, 40–53 (2009).
11. A. I. Karasevskii, "Size Effect on Thermodynamic Properties of Free Nanocrystals," Eur. Phys. J. B: Condens. Matter Complex Syst. **66**, 375–383 (2008).
12. P. M. Morse, "Diatomic Molecules According to the Wave Mechanics: II. Vibrational Levels," Phys. Rev. **34**, 57–64 (1929).
13. E. C. Marques, D. R. Sandrom, F. W. Lytle, and R. B. Greegor, "Determination of Thermal Amplitude of Surface Atoms in a Supported Pt Catalyst by EXAFS Spectroscopy," J. Chem. Phys. **77**, 1027–1034 (1982).
14. E. A. Stern, P. Livins, and Z. Zhang, "Thermal Vibration and Melting from a Local Perspective," Phys. Rev. B: Condens. Matter Mater. Phys. **43**, 8850–8860 (1991).
15. F. Baletto and R. Ferrando, "Structural Properties of Nanoclusters: Energetic, Thermodynamic, and Kinetic Effects," Rev. Mod. Phys. **77**, 371–390 (2005).

16. Yu. F. Komnik, *Physics of Metal Films: Dimensional and Structural Effects* (Atomizdat, Moscow, 1979) [in Russian].
17. Yu. I. Petrov, *Physics of Small Particles* (Nauka, Moscow, 1982) [in Russian].
18. I. D. Morokhov, V. I. Petinov, L. I. Trusov, and V. F. Petrunin, “Structure and Properties of Small Metallic Particles” Sov. Phys. Usp. **24**, 295–317 (1981).
19. W. H. Qi and M. P. Wang, “Size and Shape Dependent Lattice Parameters of Metallic Nanoparticles,” J. Nanopart. Res. **7**, 51–57 (2005).
20. N. D. Lisgarten, S. J. Peppiatt, and J. R. Samblest, “Lattice Parameter Changes in Thin Films of Bismuth,” J. Phys. C: Solid State Phys. **7**, 2263–2268 (1974).
21. K. Sumiyama and Y. Nakamura, “Lattice Expansion in Fe Films Produced by Sputtering,” Trans. Jpn. Inst. Metals **23**, 108–110 (1982).
22. I. G. Kaplan *Introduction to the Theory of Intermolecular Interactions* (Moscow: Nauka, 1982) [in Russian].
23. L. A. Girifalco and V. G. Weizer, “Application of the Morse Potential Function to Cubic Metals,” Phys. Rev. **114**, 687–690 (1959).
24. J. C. Slater, *Introduction to Chemical Physics* (McGraw Hill, New York, 1939).
25. I. M. Torrens, *Interatomic Potentials* (Academic Press, New York, 1972).
26. N. M. Kalinovskaya, I. I. Mel’nikov, and I. V. Tereshko, “Nonlinear Vibration Modeling in Hydrogen–Oxygen Atomic Chains and Water Molecular Chains,” Electronic Sci.-Tech. Journal, Vol. 5; http://www.bru.mogilev.by/science/vesnik/Papers2009/03.pdf
27. N. V. Hung, “A Method for Calculation of Morse Potential for FCC, BCC, HCP Crystals Applied to Debye-Waller Factor and Equation of State,” Commun. Phys. **14** (1), 7–14 (2004).
28. T. Luo and J. R. Lloyd, “Equilibrium Molecular Dynamics Study of Lattice Thermal Conductivity/Conductance of Au–SAM–Au Junctions;” http://arXiv.org/abs/0905.2008/pdf.
29. T. Yokoyama, K. Kobayashi, and T. Ohta, “Anharmonic Interatomic Potentials of Diatomic and Linear Triatomic Molecules Studied by Extended X-ray-Absorption Fine Structure,” Phys. Rev. B: Condens. Matter Mater. Phys. **53**, 6111–6122 (1996).
30. N. V. Hung and J. J. Rehr, “Anharmonic Correlated Einstein-Model Debye-Waller Factors,” Phys. Rev. B: Condens. Matter Mater. Phys. **56**, 43–46 (1997).
31. I. V. Pirog, I. I. Nedosekina, I. A. Zarubin, and A. T. Shuvaev, “Anharmonic Pair Potential Study in Face-Centered-Cubic Structure Metals,” J. Phys.: Condens. Matter **14**, 1825–1832 (2002).
32. M. Rieth, “Molecular Dynamics Calculations for Nanostructured Systems,” *PhD Thesis* (University of Patras, Patras, 2000).
33. W. Schommers, “The Effect of van der Waals-Type Interactions in Metals: A Pseudopotential Model,” Z. Phys. B: Condens. Matter **24**, 171–175 (1976).
34. W. Schommers, C. Mayer, H. Gobel, and P. von Blanckenhagen, “Disorder Effects at the Al(110) Surface,” J. Vac. Sci. Technol. A **13**, 1413–1415 (1995).
35. Y. Mishin, D. Farkas, M. J. Mehl, and D. A. Papaconstantopoulos, “Interatomic Potentials for Monoatomic Metals from Experimental Data and Ab Initio Calculations,” Phys. Rev. B: Condens. Matter Mater. Phys. **59**, 3393–3407 (1999).
36. G. P. Purja Pun and Y. Mishin, “Development of an Interatomic Potential for the Ni–Al System,” Philos. Mag. **89**, 3245–3267 (2009).
37. *Nano-Engineering in Science and Technology. An Introduction to the World of Nano-Design*, Series on the Foundations of Natural Science and Technology, Vol. 6 (World Scientific, Singapore, 2003).
38. A. P. Sutton and J. Chen, “Long-Range Finnis-Sinclair Potentials,” Philos. Mag. Lett. **61**, 139–146 (1990).
39. B. D. Todd and R. M. Lynden-Bell, “Surface and Bulk Properties of Metals Modeled with Sutton-Chen Potentials,” Surf. Sci. **281**, 191–206 (1993).
40. B. M. Smirnov, *Cluster Processes in Gases and Plasmas* (Wiley–VCH, Weinheim, 2010).
41. C. J. Smithells, *Metals Reference Book*, (Butterworths, London, 1967).
42. A. P. Babichev, N. A. Babushkina, A. M. Bratkovskii, et al., *Physical Quantities: A Handbook* (Energoatomizdat, Moscow, 1232) [in Russian].
43. W. B. Pearson, *A Handbook of Lattice Spacings and Structures of Metals and Alloys* (Pergamon, London, 1958).
44. *Great Soviet Encyclopedia* (Sov. Entsiklopediya, Moscow, 1969) Vols. 1–30 [in Russian].
45. B. G. Livshits, V. S. Kraposhin, and Ya. L. Linetskii, *Physical Properties of Metals and Alloys* (Metallurgiya, Moscow, 1980) [in Russian].
46. *Physical Encyclopedia* (Sov. Entsiklopediya, Moscow, 1988), Vols. 1–5 [in Russian].
47. V. N. Serezhkin and V. A. Blatov, “Coordination Numbers of Atoms and Structure of Metals,” Soros. Obrazov. Zh., No. 8, 35–39 (1999).
48. A. S. Shirinyan and Yu. S. Bilogorodskyy, “Construction of Phase Diagram of Continuous Bi–Sn Nanofilms Usig a Model of the Dependence of Energetic Parameters of Atomic Interaction on the System Size,” Metallofiz. Noveish. Tekhnol. **32**, 1493–1508 (2010).
49. A. S. Shirinyan, “Reactive Diffusion in a Binary Solid-State Nanosystem,” Phys. Solid State **52**, 1267–1275 (2010).
50. A. S. Shirinyan and Yu. S. Bilogorodskyy, “Influence of the Size Dependence of the Heterodiffusion Coefficient on Nanophase Growth in Binary Solid-Phase System,” Metallofiz. Noveish. Tekhnol. **32**, 637–654 (2010).